



How Many Lithium Ions Can Be Inserted onto Fused C₆ Aromatic Ring Systems?*

Xiaoyan Han, Guangyan Qing, Jutang Sun, and Taolei Sun*

A fundamental and persistent problem in the study of carbon-based electrode materials for lithium ion batteries is the question of how many lithium ions can be inserted onto a C₆ aromatic ring. Although different empirical models of Li_x/C₆ ($x < 3$) have been proposed, the question remains unresolved. Herein we employ 1,4,5,8-naphthalenetetracarboxylic dianhydride (NTCDA), an aromatic compound containing a naphthalene ring system (fused C₆ aromatic rings), to demonstrate that each carbon in a C₆ ring can accept a Li ion to form a Li₆/C₆ additive complex through a reversible electrochemical lithium addition reaction. This process results in Li ion insertion capacities of up to nearly 2000 mA h g⁻¹, depending on the exact molecular structure. This value is several times higher than any other organic electrode material previously reported and can be fully released under certain conditions. Our experiments and theoretical calculations indicate that the anhydride groups on the sides of the aromatic system are crucial for this process, which provides a promising strategy for the design of novel high-performance organic electrode materials.

Organic molecules^[1] are intriguing candidates for electrode materials for use in rechargeable Li ion batteries.^[2–4] The application of such species has aroused much interest recently, owing to the obvious advantages of such a system: no need for rare metals, low safety risks compared to transition metal oxides, and design flexibility at the molecular level.^[5–8] However, organic molecules are usually considered to possess relatively poor specific energies and cycling properties, as compared to those of inorganic materials, and these factors greatly limit their practical application. Recently, studies on aromatic carbonyl derivatives^[9,10] showed that organic materials can possess outstanding electrochemical performance comparable to, or even superior to, inorganic materials.^[9,11,12] Furthermore, the wide diversity of organic redox systems,^[1] as well as the excellent flexibility in their molecular design, suggest even greater prospects for these materials, and this

has inspired the exploration of new organic Li ion insertion systems with improved performance.

Aromatic C₆ rings are the basic structural units of graphite and other carbon-based electrode materials, which are the most commonly used anodes in commercial Li ion batteries owing to their high electric conductivity and low cost.^[13–15] It has traditionally been believed that each C₆ ring can accept one Li ion to form an intercalated Li/C₆ complex, giving a relatively low theoretical capacity of 372 mA h g⁻¹. Recently, studies on graphene,^[16–18] nanographene,^[19,20] and their derivatives reveal that, through the reduction of size and dimensionality, these materials exhibit unique electric and electrochemical properties superior to those of conventional graphitic materials; thus, these materials are currently a hot research topic. In studies of electrode materials for Li ion batteries,^[21,22] these derivatives also exhibit high reversible capacities of up to almost twice the theoretical value of graphite, although the detailed mechanism is still unclear.^[20–22] This leads to a fundamental question in the study of carbon-based electrode materials: How many Li ions can actually be inserted onto each C₆ aromatic ring?

Multi-ring aromatics (for example, naphthalene, NTCDA, perylene, etc.) and their derivatives have planar C₆ ring structures similar to graphene or nanographene. NTCDA is a typical example; it has a naphthalene-like ring structure consisting of two C₆ rings fused together along with two cyclic anhydride groups (Figure 1a). NTCDA is a well-known organic semiconductor with good crystallinity and has been extensively studied for use in molecular electric devices.^[23,24] It provides an ideal model to study Li ion insertion onto C₆ rings owing to the minimal number of C₆ rings it possesses, which guarantees the necessary insolubility of the electrode materials in the commonly used electrolyte solution (ethylene carbonate/dimethyl carbonate/LiPF₆) for Li ion batteries. NTCDA also possesses the necessary degree of conductivity for electron transport among molecules. We investigated the electrochemical Li ion insertion/deinsertion properties of NTCDA using model test cells with Li metal as the counter electrode. The working electrode consisted of NTCDA, acetylene black (AB), and polytetrafluoroethylene binders in a weight ratio of about 60:35:5.

The cells were initially cycled by discharging (Li ion insertion) and charging (Li ion deinsertion) repeatedly in a potential range of 0.001–3.0 V vs. Li/Li⁺ at a moderate current rate of 100 mA g⁻¹. Figure 1b shows selected discharge/charge curves (the 1st, 2nd, 3rd, and 8th cycles) for NTCDA.^[33] Figure 1c shows the corresponding discharge and charge capacities of NTCDA versus the cycle number. The first discharge and charge capacities are 1273 and 724 mA h g⁻¹, respectively, showing a coulombic efficiency

[*] X. Han, G. Qing, T. Sun

State Key Laboratory of Advanced Technology for Materials Synthesis and Processing, Wuhan University of Technology
Wuhan, 430070 (China)
E-mail: suntaolei@iccas.ac.cn

J. Sun

College of Chemistry and Molecular Sciences, Wuhan University
(China)

[**] This work was supported by the National Science Foundation of China (51073123, 51173142, 91127027). The authors also thank Dr. Jie Li in Muenster University for her help in the analysis of EIS data.



Supporting information for this article is available on the WWW under <http://dx.doi.org/10.1002/anie.201109187>.

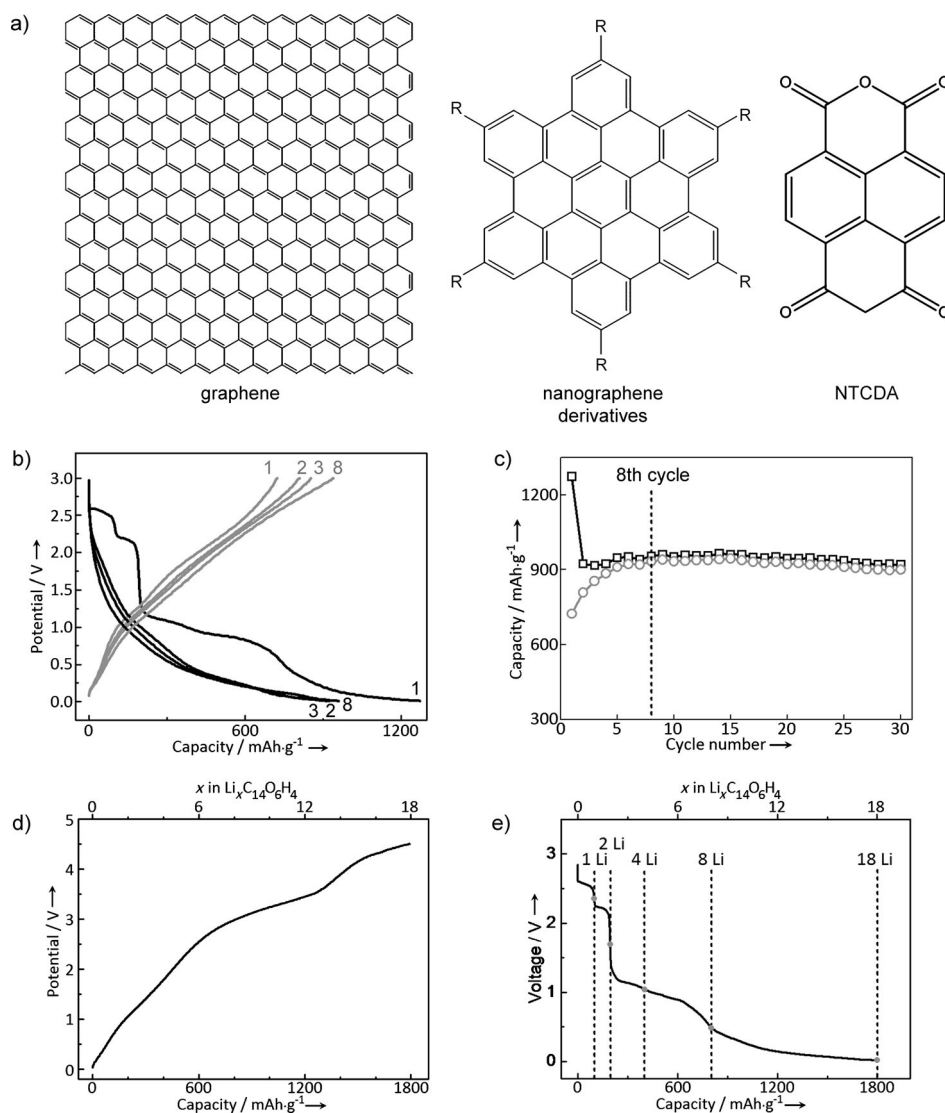


Figure 1. a) A comparison of the planar C₆ ring structures for graphene, nanographene derivatives, and NTCDA. b–d) Electrochemical performance of NTCDA. b) Potential profiles for the initial discharge/charge cycles; discharge (—), charge (---). c) Discharge/charge capacity curves versus cycle number. Current rate: 100 mA h g⁻¹; discharge (—□—), charge (—○—). d) Potential profile of further charge experiments after 30 cycles using a current rate of 50 mA g⁻¹. e) Potential profile of the discharge experiment of NTCDA using a current rate of 20 mA g⁻¹. The profile exhibits five distinct discharge plateaus, which correspond to the insertion of 1, 2, 4, 8, and 18 Li ions. The corresponding discharge potentials are 2.34 V, 1.69 V, 1.04 V, 0.47 V, and 0.001 V, respectively (indicated by grey dots). All data were obtained after subtracting the corresponding contribution by AB.

(CE) of about 57%. In the second cycle, the values change to 923 and 809 mA h g⁻¹, respectively, with a CE of about 88%. With further cycles, the discharge capacity does not change significantly, while the charge capacity continues to gradually increase, reaching a maximum value of about 933 mA h g⁻¹ (CE = 98%) in the eighth cycle. The charge capacity then slowly decreases to about 899 mA h g⁻¹ by the 30th cycle (CE remains at 98%).

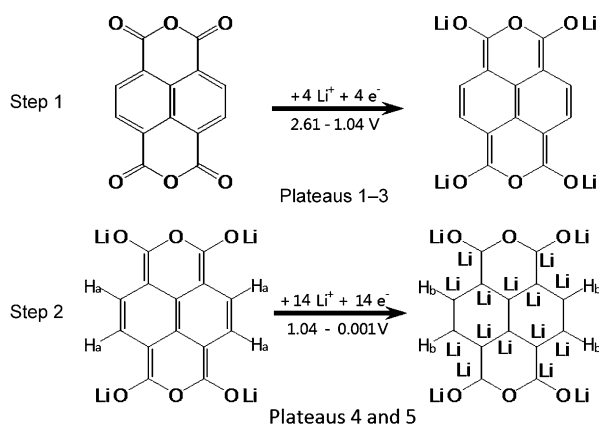
The above data illustrate the excellent reversible capacity of NTCDA. These values are several times higher than that of previously reported organic materials, which are usually lower than 300 mA h g⁻¹.^[7] During the initial seven cycles, it was also noted that the quantities of Li ion insertion are

significantly higher than those of Li ion deinsertion. From the eighth cycle onward, the coulombic efficiencies become stable and exceed 98%. This suggests that the inserted Li ions may gradually accumulate before the eighth cycle, after which the Li ions inserted and released in each cycle are almost equal, allowing for circuit loss. The amount of accumulated Li ions after the discharge process of the eighth cycle can be calculated by summing the difference between discharge capacities and charge capacities for cycles one through seven and the discharge capacity of the eighth cycle, which amounts to about 1803 mA h g⁻¹. When we further charged the cells using a smaller current rate (50 mA g⁻¹), a maximum charge capacity of 1793 mA h g⁻¹ was observed (Figure 1d), which is within experimental error of the above calculated amount of accumulated Li ions. These results show that the accumulated Li ions can be completely released under the experimental conditions, indicating that there is almost no dead capacity in this kind of material.

To investigate the maximum amount of Li ion insertion in a single discharge process, smaller current rates were applied. Figure 1e shows the discharge curve at a current rate of 20 mA g⁻¹. It gives a discharge capacity of 1804 mA h g⁻¹, which is almost the same as the maximum amount of accumulated Li ions (1803 mA h g⁻¹) determined above. When the discharge current is further reduced to 10 mA g⁻¹, the capacity does not increase accordingly. Therefore, it can be inferred that the largest amount of Li ion insertion in a single discharge process is around 1800 mA h g⁻¹. Considering that for one molecule of NTCDA one Li ion insertion contributes a theoretical capacity of 100 mA h g⁻¹, the above data show that each NTCDA molecule is capable of accepting 18 Li ions. Moreover, it can be seen in Figure 1e that there are five distinct discharge plateaus, which correlate to the insertion of 1, 2, 4, 8, and 18 Li ions per molecule. The corresponding discharge potentials are 2.34 V, 1.69 V, 1.04 V, 0.47 V, and 0.001 V, respectively. In cyclic voltammetry (CV) measurements employing a three-electrode system, five distinct reduction

peaks were observed in the initial half cycle. The voltages of these peaks are in good agreement with the five discharge plateaus (Supporting Information, Figure S1).

According to our previous study,^[9] the initial four Li ions inserted at a potential of above 1.04 V can be attributed to a lithium enolization reaction at the four carbonyl oxygens of NTCDA. For the other 14 Li ions, we believe that they may be inserted by an electrochemical reaction on the unsaturated carbons of the C₆ and anhydride ring systems, which total exactly 14. Based on this assumption, the possible electrochemical process for Li ion insertion may be as shown in Scheme 1. It includes two major steps: the addition of lithium through enolization of the carbonyl groups at potentials above 1.04 V (plateaus 1–3), and then the electrochemical lithium addition reaction to the unsaturated carbons to form 1:1 Li/C complexes at potentials below 1.04 V (plateaus 4–5).



Scheme 1. Proposed electrochemical insertion of Li ions onto NTCDA during the discharge process. See text for details.

As Li ion insertion will induce a change in the crystalline state of the electrode materials, an X-ray diffraction (XRD) study was performed to investigate the crystal structure changes in NTCDA at different discharge plateaus. As shown in Figure S2 in the Supporting Information, the sample exhibits good crystallinity after the first discharge plateau (2.34 V), although the transformation of the crystal structure from the insertion of the first Li ion leads to diffraction peaks that are much different from those of pristine NTCDA. After the second discharge plateau (1.69 V), the sample still retains a certain degree of crystallinity, although the crystallinity has decreased significantly from that of the first plateau. However, when discharge potentials decrease to 1.04 V and below (3rd, 4th, and 5th plateaus), no obvious diffraction peaks can be observed, which is indicative of the formation of amorphous phases. These results are consistent with the addition process proposed in Scheme 1, because initial Li ion insertion onto the side groups will not damage the planar conjugated structure of the molecules, which helps to preserve the crystallinity of the sample. On the other hand, Li ion insertion onto the C₆ rings will destroy the conjugation and planarity of the molecules, resulting in the collapse of the crystal structure.

An NMR study was also conducted to get more information on the structural changes of the molecules. Figure 2a shows ¹H NMR spectra for pristine NTCDA and after each of the five discharge plateaus (2.34 V, 1.69 V, 1.04 V, 0.47 V, and

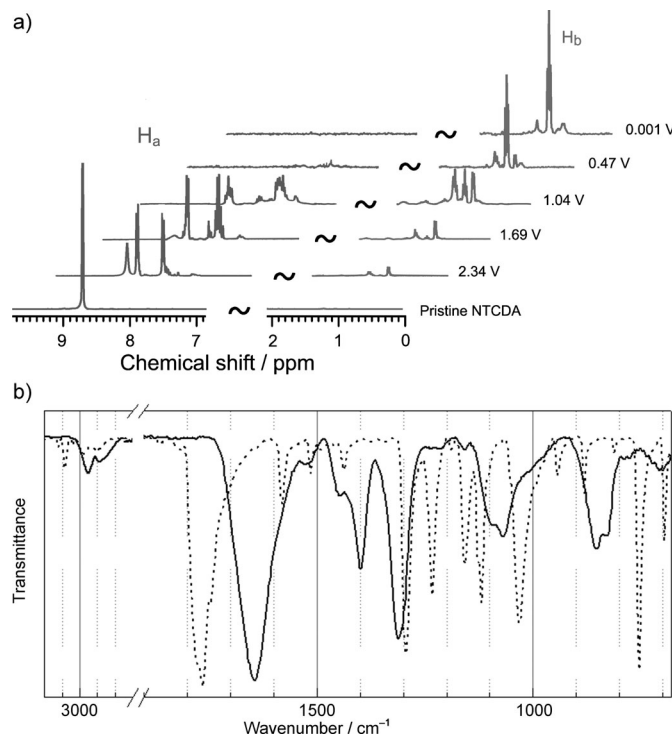


Figure 2. ¹H NMR spectra (a) and IR spectra (measured in vacuum) of NTCDA (b) before and after discharge. a) The spectra were recorded after the discharge plateaus at 2.34 V, 1.69 V, 1.04 V, 0.47 V, and 0.001 V. See text for details. b) Pristine NTCDA (-----), NTCDA after being discharged to 0.001 V (—). See text for details.

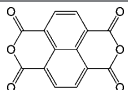
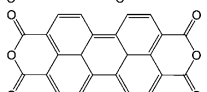
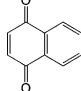
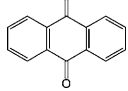
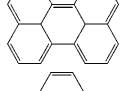
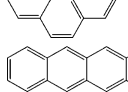
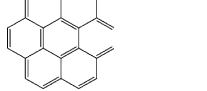
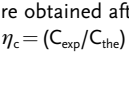
0.001 V, respectively). As all four protons on NTCDA are identical (denoted as H_a), the original sample before discharge exhibits a single strong signal with a chemical shift of $\delta = 8.7$ ppm. It gradually shifts and splits into multiple peaks in the range of $\delta = 7.4$ –8.6 ppm (Figure 2a, left side) along with the decrease in discharge potential observed after the initial three plateaus. These results reflect the destruction of the symmetry of the aromatic system, resulting in different chemical environments for each proton. When the discharge potential decreases further to 0.47 V and then 0.001 V (after the 4th and 5th plateaus), these peaks almost completely disappear, showing that there are no longer aromatic protons in the molecules. These changes are accompanied by the appearance and growth of a new signal in the high field region with a chemical shift of $\delta = 0.7$ –1.4 ppm (Figure 2a, right side; external contaminants were strictly precluded), which are attributed to protons on saturated carbons (denoted as H_b). The ratios of the integrated areas for the H_a and H_b signals (I_A/I_B) are 11.1, 6.7, 1.2, 0.1, and 0.0, respectively, after the five discharge plateaus. These results clearly demonstrate the transformation of the NTCDA framework from an aromatic state to a saturated state, which is consistent with the XRD

results and supports the proposal in Scheme 1. This process is somewhat similar to the reversible hydrogenation reaction on graphene reported by Elias et al.^[25] This transformation was also supported by comparing the IR spectra (Figure 2b) of pristine NTCDA with the sample after discharge to 0.001 V, in which the disappearance of the characteristic bands for aromatic rings (both C=C and C-H) and the appearance of saturated C-H bands could be clearly observed (see Figure S3 and Table S1 in the Supporting Information for details). Correspondingly, this process leads to an impedance change in NTCDA as the discharge process proceeds, as shown by electrochemical impedance spectroscopy (EIS)^[26,27] measurements (Supporting Information, Figures S4 and S5). When the sample was again charged to 3.0 V and 4.8 V, the H_b signal disappeared and the H_a signal reappeared (Supporting Information, Figure S8), which clearly demonstrates the reversibility of this redox process.

To check whether this process only occurs in NTCDA, other multi-ring aromatic compounds and their derivatives were also tested in discharge experiments under the same conditions. As summarized in Table 1 (see Figure S6 in the Supporting Information for electrochemical performance details), 3,4,9,10-perylenetetracarboxylic dianhydride (PTCDA) also exhibits a large discharge capacity (C_{exp} ; 1925 mA h g⁻¹), which is almost equal to its theoretical value (C_{the}), within experimental error. However, for the other two aromatic compounds with carbonyl groups (1,4-naphthoquinone (NQ) and anthraquinone), the performance efficiency (η_c ; $\eta_c = (C_{\text{exp}}/C_{\text{the}}) \times 100$) values are 37.9% and 33.8%, respectively. For compounds without carbonyl groups, such as perylene, pyrene, pentacene, and coronene, the experimental capacities are very low compared to their theoretical values ($\eta_c = 15\text{--}23\%$). In a previous study, Koch et al. had similarly reported that anhydride, carbonyl, or carboxyl groups produced by oxidation on the edges of graphite layers could improve the capacity performance of graphite to some extent,^[28] although the improvement was relatively limited (for example, from 370 to 430 mA h g⁻¹). These results show that anhydride groups, or other carbonyl-containing groups in the conjugated system, play crucial roles in the process of Li ion insertion onto C₆ rings. This analysis is supported by density functional theory (DFT) calculations^[29,30], which indicate that the stepwise Li ion insertion reaction for compounds with anhydride groups, such as NTCDA, shows significantly lower free energy than for unsubstituted aromatics, such as pyrene and naphthalene (Figure 3).

The above results clearly demonstrate a novel Li ion insertion model that differs significantly from other mechanisms for organic compounds and provides a Li ion insertion capacity several times higher than any previously reported. Our study also challenges the interlayer model for Li ion insertion onto compounds such as graphite by showing that Li ions can be inserted onto C₆ rings in a different way. This may explain why many carbon-based materials, especially those with imperfect structures, such as porous carbon materials,^[31] fibrous carbon materials,^[32] and other materials for which different Li_x/C_6 ($1 < x < 3$) intercalation results have been reported, exhibit much higher practical capacities than the

Table 1: A comparison between the theoretical (C_{the}) and experimental (C_{exp}) specific capacity for selected multi-ring aromatic compounds.

Entry	Compound name	Molecular structure	C_{the} [mA h g ⁻¹]	C_{exp} ^[a] [mA h g ⁻¹]	η_c ^[b] [%]
1	NTCDA		1800	1804	100 ^[c]
2	PTCDA		1913	1925	100 ^[c]
3	NQ		2034	711	37.9
4	anthraquinone		2060	696	33.8
5	perylene		2125	479	22.6
6	pyrene		2120	478	22.5
7	pentacene		2119	482	22.8
8	coronene		2142	321	15.0

[a] All capacity data were obtained after subtracting the corresponding contribution of AB. [b] $\eta_c = (C_{\text{exp}}/C_{\text{the}}) \times 100$. [c] The listed values are approximate.

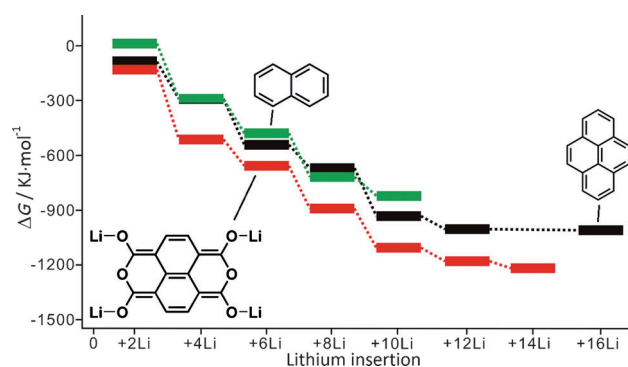


Figure 3. Reaction free energy (ΔG) for lithium addition onto the aromatic rings of NTCDA (red), pyrene (black), and naphthalene (green). Data obtained from quantum chemical DFT calculations, with ΔG values determined by subtracting the minimized energies of the products at each level of lithium insertion from those of the corresponding starting compounds and lithium. For NTCDA, the starting compound is NTCDA after the initial insertion of four Li ions onto the carbonyl groups (after step 1), as shown.

theoretical value of graphite. Our study also reveals that the presence of higher oxidation states of carbon, for example, anhydrides or carbonyl groups on C₆ rings, plays a crucial role in this reaction. It points to a promising approach for further improvement in the capacity of carbon-based materials.

Moreover, this electrochemical lithium addition to C₆ rings is thoroughly reversible, as was demonstrated by the discharge/charge cycle experiment, which is also important for practical applications.

In conclusion, we have reported a novel Li ion insertion model for organic electrode materials for use in rechargeable Li ion batteries, based on reversible electrochemical lithium addition to C₆ aromatic rings. Our study indicates that each C₆ ring can reversibly accept 6 Li ions to form a 1:1 Li/C complex, giving discharge capacities of up to nearly 2000 mAh g⁻¹, which is several times higher than those of other organic models. Our results answer a fundamental question in the study of carbon-based electrode materials: How many Li ions can be inserted onto a C₆ ring? This work also provides important insights for the future development of high-performance organic electrode materials.

Received: December 28, 2011

Published online: April 18, 2012

Keywords: aromaticity · carbon-based materials · ion–molecule reactions · lithium · organic electrodes

- [1] P. Novák, K. Müller, K. S. V. Santhanam, O. Haas, *Chem. Rev.* **1997**, 97, 207–282.
- [2] C. Liu, F. Li, L. P. Ma, H. M. Cheng, *Adv. Mater.* **2010**, 22, E28–E62.
- [3] J. B. Goodenough, Y. Kim, *Chem. Mater.* **2010**, 22, 587–603.
- [4] J. M. Tarascon, M. Armand, *Nature* **2001**, 414, 359–367.
- [5] T. Le Gall, K. H. Reiman, M. C. Grossel, J. R. Owen, *J. Power Sources* **2003**, 119, 316–320.
- [6] K. Nakahara, J. Iriyama, S. Iwasa, M. Suguro, M. Satoh, E. J. Cairns, *J. Power Sources* **2007**, 165, 398–402.
- [7] M. Armand, S. Grugeon, H. Vezin, S. Laruelle, P. Ribière, P. Poizot, J. M. Tarascon, *Nat. Mater.* **2009**, 8, 120–125.
- [8] W. Walker, S. Grugeon, O. Mentre, S. Laruelle, J. M. Tarascon, F. Wudl, *J. Am. Chem. Soc.* **2010**, 132, 6517–6523.
- [9] X. Han, C. Chang, L. Yuan, T. Sun, J. Sun, *Adv. Mater.* **2007**, 19, 1616–1621.
- [10] H. Y. Chen, M. Armand, M. Courty, M. Jiang, C. P. Grey, F. Dolhem, J.-M. Tarascon, P. Poizot, *J. Am. Chem. Soc.* **2009**, 131, 8984–8988.
- [11] B. Z. Jang, C. G. Liu, D. Neff, Z. N. Yu, M. C. Wang, W. Xiong, A. Zhamu, *Nano Lett.* **2011**, 11, 3785–3791.
- [12] S. W. Lee, N. Yabuuchi, B. M. Gallant, S. Chen, B. S. Kim, P. T. Hammond, Y. Shao-Horn, *Nat. Nanotechnol.* **2010**, 5, 531–537.
- [13] M. Endo, C. Kim, K. Nishimura, T. Fujino, K. Miyashita, *Carbon* **2000**, 38, 183–197.
- [14] H. Li, Z. Wang, L. Chen, X. Huang, *Adv. Mater.* **2009**, 21, 4593–4607.
- [15] F. Cheng, Z. Tao, J. Liang, J. Chen, *Chem. Mater.* **2008**, 20, 667–681.
- [16] K. S. Novoselov, A. K. Geim, S. V. Morozov, D. Jiang, Y. Zhang, S. V. Dubonos, I. V. Grigorieva, A. A. Firsov, *Science* **2004**, 306, 666–669.
- [17] V. P. Gusynin, S. G. Sharapov, *Phys. Rev. Lett.* **2005**, 95, 146801.
- [18] D. H. Wang, R. Kou, D. Choi, Z. G. Yang, Z. M. Nie, J. Li, L. V. Saraf, D. H. Hu, J. G. Zhang, G. L. Graff, J. Liu, M. A. Pope, I. A. Aksay, *ACS Nano* **2010**, 4, 1587–1595.
- [19] A. Tracz, J. K. Jeszka, M. D. Watson, W. Pisula, K. Müllen, T. Pakula, *J. Am. Chem. Soc.* **2003**, 125, 1682–1683.
- [20] S. Yang, X. Feng, L. Zhi, Q. Cao, J. Maier, K. Müllen, *Adv. Mater.* **2010**, 22, 838–842.
- [21] D. H. Wang, D. W. Choi, J. Li, Z. G. Yang, Z. M. Nie, R. Kou, D. H. Hu, C. M. Wang, L. V. Saraf, J. G. Zhang, I. A. Aksay, J. Liu, *ACS Nano* **2009**, 3, 907–914.
- [22] M. Liang, L. Zhi, *J. Mater. Chem.* **2009**, 19, 5871–5878.
- [23] S. R. Forrest, *Chem. Rev.* **1997**, 97, 1793–1896.
- [24] C. K. Chan, E. G. Kim, J. L. Brédas, A. Kahn, *Adv. Funct. Mater.* **2006**, 16, 831–837.
- [25] D. C. Elias, R. R. Nair, T. M. G. Mohiuddin, S. V. Morozov, P. Blake, M. P. Halsall, A. C. Ferrari, D. W. Boukhvalov, M. I. Katsnelson, A. K. Geim, K. S. Novoselov, *Science* **2009**, 323, 610–613.
- [26] E. J. Barsoukov, R. Macdonald, *Impedance spectroscopy theory, experiment, and applications*, Vol. 2, Wiley, Hoboken, **2005**.
- [27] L. J. Xue, Y. F. Xu, L. Huang, F. S. Ke, Y. He, Y. X. Wang, G. Z. Wei, J. T. Li, S. G. Sun, *Electrochim. Acta* **2011**, 56, 5979–5987.
- [28] Y. Ein-Eli, V. R. Koch, *J. Electrochem. Soc.* **1997**, 144, 2968–2973.
- [29] H. Tachikawa, A. Shimizu, *J. Phys. Chem. B* **2005**, 109, 13255–13262.
- [30] Y. Wang, P. B. Balbuena, *Int. J. Quantum Chem.* **2005**, 102, 724–733.
- [31] Y. S. Hu, P. Adelhelm, B. M. Smarsly, S. Hore, M. Antonietti, J. Maier, *Adv. Funct. Mater.* **2007**, 17, 1873–1878.
- [32] S. H. Yoon, C. W. Park, H. J. Yang, K. Korai, I. Mochida, R. T. K. Baker, N. M. Rodriguez, *Carbon* **2004**, 42, 21–32.
- [33] All the capacity data and curves reported in this work were obtained after subtracting the contribution of acetylene black (AB).